

Research paper

Removal of Methylene Blue from aqueous solutions by adsorption on Kaolin: Kinetic and equilibrium studies



Lotfi Mouni^{a,*}, Lazhar Belkhiri^b, Jean-Claude Bollinger^c, Abdelkrim Bouzaza^d, Aymen Assadi^d, Amar Tirri^b, Farid Dahmoune^e, Khodir Madani^e, Houcine Remini^e

^a Laboratoire de Gestion et Valorisation des Ressources Naturelles et Assurance Qualité, Faculté SNVST, Université Akli Mohand Oulhadj, Bouïra 10000, Algeria

^b Département d'Hydraulique, Université de Batna, 05000, Algeria

^c Groupement de Recherche Eau-Sol-Environnement (GRESE), Université de Limoges, 123 Avenue Albert Thomas, 87060 Limoges, France

^d Laboratoire Sciences Chimiques de Rennes – Equipe Chimie et Ingénierie des Procédés, UMR 6226 CNRS, ENSCR, Avenue du Général Leclerc, 35700 Rennes, France

^e Research laboratory of Biomathematics Biochemistry, Biophysics and Scientometrics, Université de Bejaia, 06000 Bejaia, Algeria

ARTICLE INFO

Keywords:

Kaolin
Adsorption
Methylene Blue
Kinetics

ABSTRACT

Removal of Methylene Blue (MB) from aqueous solutions is studied using a raw Algerian kaolin sample as a low-cost adsorbent. The effects of pH, contact time, dye concentration and temperature are all taken into consideration. The adsorption kinetics results are adjusted to best fit the pseudo-second order model. The experimental data are analyzed by Langmuir isotherms, revealing that the maximum adsorption capacity of MB on this kaolin sample equals 52.76 mg/g at $T = 25\text{ }^{\circ}\text{C}$ and $\text{pH} = 6.0$. The calculated thermodynamic data demonstrates that adsorption is spontaneous and enhanced at higher temperatures. Desorption studies with water indicate that the adsorbent could successfully retain MB, even after four cycles. From these results, it can be considered that the raw Algerian kaolin sample tested herein is effective in the removal of MB from aqueous solutions and moreover may be used as an alternative to high-cost commercial adsorbents.

1. Introduction

The textile industry is the major source of dyes and generates colored wastewater that is capable of causing severe water pollution. According to Allègre et al. (Allègre et al., 2006), dyeing 1 kg of cotton with reactive dyes requires an average of 70–150 L water, 0.6 kg NaCl and 40 g reactive dye. > 80,000 metric tons of reactive dyes are produced and consumed each year, but up to 20%–30% of these applied dyes (approx. 2 g/L) is not fixed to the fabric and thus contributes to the coloration and toxicity of the effluent. Such wastewater is commonly associated with a high pH (10–11) and temperature (50°–70 °C). Colored dye effluents are generally considered to be toxic to the animal and plant life of a particular region and habitat (Walsh et al., 1980). Moreover, almost all dyes are poorly biodegradable or resistant to environmental conditions and, therefore, create major problems in the treatment of wastewater stemming from the dyeing industry (Hao et al., 2000). As a final consideration, dyes cannot be completely removed by means of conventional biological treatment processes, such as activated sludge and anaerobic digestion: due to their low biodegradability, nearly 90% of reactive dyes remain unchanged after undergoing an activated sludge process. Several physicochemical technologies,

including coagulation/flocculation, membrane separation, ion exchange, chemical oxidation, electrochemical techniques, adsorption and photocatalysis, have been studied for the purpose of removing dye from wastewater (Marrot and Roche, 2002; Allègre et al., 2006; Holkar et al., 2016).

Compared with the methods cited above, the adsorption of dyes from aqueous solution has proven to be an excellent approach to treating effluents as well as a cost-effective technique. After the seminal paper by Crini in 2006 (Crini, 2006), several reviews have compiled works dedicated to removing exhausted dyes from effluent water using low-cost adsorbents, e.g. natural minerals or biological species, agricultural byproducts, wastes from various industrial processes (Mondal, 2008; Gupta and Suhas, 2009; Rodríguez et al., 2012; Yagub et al., 2014; Ngulube et al., 2017). Adsorption kinetics describes the decrease in aqueous adsorbate concentration from solution versus reaction time variation. During the adsorption process, four distinct steps are considered: i) transport of the aqueous adsorbate to the film surrounding the adsorbent particle surface (this first step can be neglected if the system has been perfectly stirred); ii) external diffusion; iii) intra-particle diffusion; and iv) physical or chemical surface reactions (Gadd, 2009).

* Corresponding author.

E-mail address: lotfimouni@gmail.com (L. Mouni).

Clay minerals act as good adsorbents owing to their high cation exchange capacity and high specific surface areas relative to their small particle size; moreover, these minerals offer the advantage of being abundant and available at lower cost. Their surface reactions therefore produce strong biochemical and ecological effects on soils and water, hence justifying use of these materials in decontamination and remediation treatments (Quintelas et al., 2011; Sánchez-Jiménez et al., 2012). Kaolin is the most abundant mineral in soils and sediments; it interacts with other soil elements in contributing to the mechanical stability of the soil column (Chen et al., 2000). Kaolin has been widely used in: ceramics manufacturing (Bouzerara et al., 2009; Schroeder and Erickson, 2014), dye adsorption (Harris et al., 2001), pesticides (Sanchez-Martin et al., 2006), metal ions (Gupta and Bhattacharyya, 2012), and oil well drilling due to its rheological properties (Au and Leong, 2013).

Methylene Blue (MB), a cationic dye, was selected herein because of its widespread application in textile dyeing and by virtue of being present in the human and veterinary pharmacopoeia for a long time (DiSanto and Wagner, 1972; Oz et al., 2010). Another well-known use of MB adsorption pertains to the determination of surface properties in either (hydrated) clays or activated carbon materials (Hang and Brindley, 1970; Raposo et al., 2009). The removal of Methylene Blue, one of the most extensively applied textile dyes, from aqueous media has recently been reviewed by Kannan and Sundaram (Kannan and Sundaram, 2001) for activated carbon, and by Rafatullah et al. (Rafatullah et al., 2010) for various kinds of low-cost adsorbents.

This article will present the results obtained from experimental investigations performed on MB adsorption with a low-cost sorbent, i.e. natural raw (Algerian) kaolin, denoted here as KT3B. The effects of contact time, initial dye concentration, temperature, pH and adsorbent dosage on the static adsorption of the dye onto the KT3B kaolin sample will all be examined. The pseudo-first order and pseudo-second order models will be introduced to correlate the adsorption kinetics data of MB onto kaolin. Also, the equilibrium data will be analyzed using the Langmuir isotherm model and the adsorption thermodynamics will be evaluated. Moreover, the reuse of kaolin after MB desorption will be assessed in order to minimize the method's economic cost. This fundamental study will prove helpful for subsequent application in designing an adsorber for the treatment of dye-containing effluent discharged by the textile industry.

2. Materials and methods

2.1. Materials

The Tamazert kaolin deposit is located about 60 km north of the town of Jijel, in Eastern Algeria. A kaolin material originating from Tamazert, and industrially treated with sodium carbonate, was supplied by ENOF Ltd. (Algeria). The material was not ground because its grain size was already adequate for test purposes (i.e. $\leq 60 \mu\text{m}$); it was only air dried, first at ambient temperature (25 °C) then at 110 °C in an oven. This raw kaolin sample will be denoted KT3B in the following discussion.

Methylene Blue (MB, or tetramethylthionine chloride, Fig. 1; CAS Number: 122965-43-9; Color Index number CI-52015), supplied by Panreac (Spain), was selected as an adsorbate and not purified prior to use. The MB molecular properties are: molar mass (319.85 g/mol),

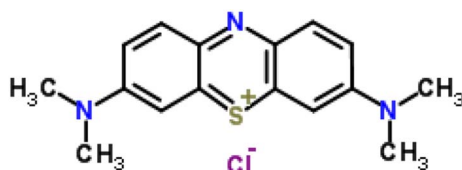


Fig. 1. The chemical structure of MB.

molar volume (241.9 cm³/mol), width (14.3 Å), depth (6.1 Å), thickness (4 Å), and molecular diameter (0.8 nm), according to the evaluations conducted by Pelekani and Snoeyink (Pelekani and Snoeyink, 2000).

2.2. Characterization

The cation exchange capacity (CEC) of the KT3B sample was determined by relying on BaCl₂-triethanolamine (Primo-Yúfera and Carrasco Dorrién, 1981). The specific surface area (SSA) of the KT3B sample (previously outgassed at 200 °C for 8 h under 0.1 Torr vacuum) was determined by N₂ adsorption at 77 °K using a Micromeritics ASAP 2020 analyzer. The particle size distribution was measured with the MICRO-P laser granularity instrument (Malvern Instruments Ltd.).

An X-ray diffraction (XRD) analysis of the samples was carried out with a Powder X-ray Diffractometer (Bruker AXS) in the 2 θ angle ranging from 2° to 65° incremented by a 0.025° step. A scanning electron microscopy (SEM) analysis of the samples was performed using a Philips SEM-505 scanning electron microscope, operated at 300 kV/SE and 50° inclination. We also made use of an Olympus BX50 polarizing microscope.

To estimate the pH of KT3B dispersion, the following procedure was adopted (Pansu and Gautheyrou, 2003): a 2:1 (v:w) water:KT3B dispersion was prepared and shaken for 24 h at 30 °C (Labwit ZWY-304); after 24 h, the dispersion was filtered through a Millipore 0.45 μm (Z227366 - Millex syringe filter units); and the pH of the filtrate was determined with a Jenway 3010 digital pHmeter. The FTIR spectra were obtained using a Spectrum GX spectrometer (Perkin-Elmer) at a 4 cm⁻¹ resolution: undiluted KT3B samples in powder form were scanned and recorded between 4000 and 400 cm⁻¹.

Chemical components were obtained by dry chemical analysis. Real density (volumetric mass) was measured according to the pycnometric method. The loss on ignition (LOI) was determined by weighing the sample in a crucible both before and after overnight heating at 100 °C in a muffle furnace in order to remove water.

The point of zero charge (PZC) of the KT3B was determined (Noh and Schwarz, 1989) by applying a solid-to-liquid ratio of 1:1000. To carry this step out, 0.1 mg of KT3B was added to 100 mL of water at pH varying from 2 to 12 (adjusted with concentrated HNO₃ and NaOH) and then stirred for 24 h. Some of the physicochemical properties of the KT3B kaolin sample are presented in Table 1.

2.3. Analysis of Methylene Blue concentration

Methylene Blue (C₁₆H₁₈ClN₃S·2H₂O, MB) was selected as the adsorbate species. The dye stock solutions were prepared by dissolving accurately weighted dye powder in Milli-Q water at a concentration of 1000 mg/L. The experimental solutions were derived by diluting the dye stock solutions in precise proportions to different initial concentrations. The pH of these solutions was adjusted to the desired value

Table 1
Composition of the raw kaolin sample KT3B.

Component	Content (mass%)
SiO ₂	48.60
Al ₂ O ₃	33.90
TiO ₂	0.04
CaO	0.06
MgO	0.032
Fe ₂ O ₃	0.90
Na ₂ O	0.08
K ₂ O	2.70
P ₂ O ₅	0.14
MnO	0.35
LOI ^a	10.80

^a Loss on ignition.

by adding a small quantity of 0.1 mol/L HCl and/or 0.1 mol/L NaOH. The MB concentration in the supernatant solution before and after adsorption was determined using a UV spectrophotometer (Shimadzu UV Mini-1240) at 663 nm. The calibration curve was highly reproducible and linear over the concentration range targeted by this work (i.e. from 2 to 80 mg/L). All experiments were carried out in triplicate, with all data being calculated and the average values taken to represent the result.

2.4. Adsorption studies

Batch adsorption experiments were performed in a set of Erlenmeyer flasks (250 mL), each of which contained 100 mL of different MB concentrations (80–250 mg/L) along with 50 mg of adsorbent. An orbital shaker (Labwit ZWY-304) was introduced at a desired temperature and pH. To reach steady-state adsorption, a time contact equal to 180 min was set for all experiments. After 180 min, the dispersion was filtrated with Millipore 0.45 μm (Millex syringe filter units) and the filtrate was analyzed by UV/visible spectrophotometry at $\lambda = 663 \text{ nm}$.

Equilibrium experiments were conducted for various times, while the pH was gradually adjusted by adding small amounts of diluted HCl or NaOH solutions (0.1 mol/L). The adsorbed amount of MB at equilibrium was calculated by the following equation:

$$q_e = (C_0 - C_e) \times V/m \quad (1)$$

where q_e (mg/g) denotes the equilibrium adsorption capacity of MB adsorbed per gram of the KT3B, C_0 and C_e (mg/L) the initial and equilibrium MB concentrations respectively, V the volume of the MB solution (L), and m the kaolin mass (g). Each experiment was performed at least in duplicate under identical conditions. Two separate tests showed that the standard deviation of the measurement equaled $\pm 2.0\%$. The adsorption percentage (% removal) of MB from aqueous solution can be calculated as follows:

$$\text{Removal percentage} = 100 \times (C_0 - C_e)/C_0 \quad (2)$$

2.5. Desorption experiments

First of all, the kaolin was heavily loaded with MB by mixing 0.1 g of the KT3B sample with 100 mL of the dye solution (80 mg/L); the mixture was shaken for 2 h. The KT3B loaded with MB was separated by filtration and then mixed several times with 100 mL of distilled water on the orbital shaker; the concentrations of MB in the eluate were determined in order to investigate desorption efficiency.

2.6. Error analysis

Each experiment or analysis was at least duplicated, often triplicated; in all figures, the size of symbols includes the standard deviation from experimental data (3% to 5%).

The unknown constants in the model equations for kinetics and isotherm studies were obtained using nonlinear least-squares (NLLS) data processing with the Origin 8.0 software at the 95% confidence level.

In these single-component isotherm studies, the optimization procedure requires an error function to be defined in order to evaluate the fit of the isotherm equation to the experimental equilibrium data. In this study, the linear coefficient of determination (R^2), the non-linear Chi-square test (χ^2) and the root mean square error (RMSE) statistical tests were all performed for both the kinetics and isotherm models. The corresponding mathematical equations are then:

$$\chi^2 = \sum (q_{e,exp} - q_{e,calc})^2 / q_{e,calc} \quad (3)$$

$$\text{RMSE} = [\sum (q_{e,exp} - q_{e,calc})^2 / n]^{1/2} \quad (4)$$

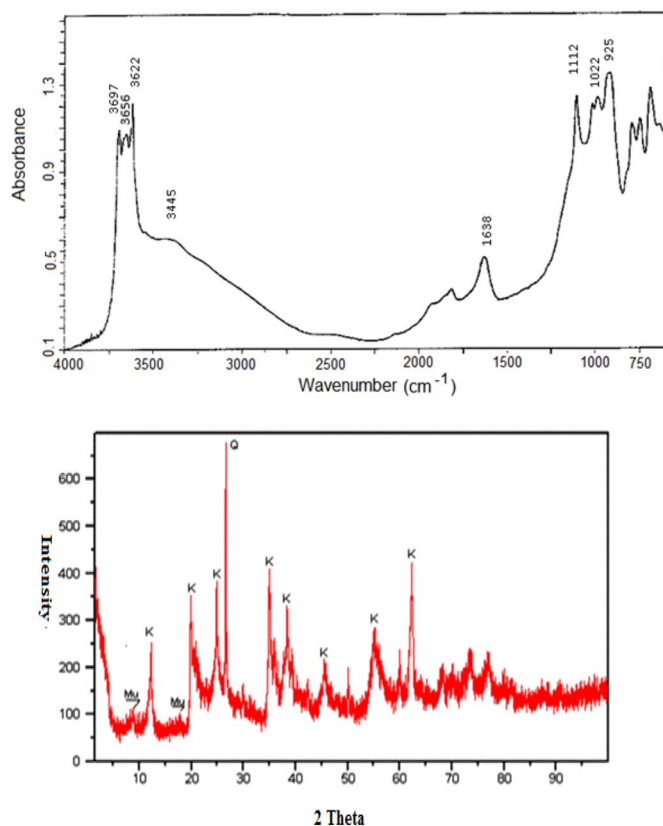


Fig. 2. XRD and FTIR spectrum of KT3B (Q: quartz; K: kaolin).

where $q_{e,exp}$ ($\text{mg}\cdot\text{g}^{-1}$) is the experimental data of the equilibrium capacity, and $q_{e,calc}$ ($\text{mg}\cdot\text{g}^{-1}$) the equilibrium capacity obtained from model calculations. If the model data are similar to the experimental data, then χ^2 will be a smaller number; if they differ, χ^2 will be a higher one. It is necessary therefore to analyze the data using the non-linear Chi-square test so as to confirm the best-fit isotherm for this adsorption system (Vimonses et al., 2009).

3. Results and discussion

3.1. Characterization of the KT3B kaolin sample

The chemical composition of the KT3B sample used for sorption experiments is provided in Table 1. The material analysis has revealed that the sample contained mainly silica and alumina, which accounted for 82.5% of the total mass. The X-ray diffraction of this KT3B raw sample indicated the presence of quartz (12.36%) and kaolinite (61.78%) as major phases (Fig. 2). Kaolinite is a well-defined, naturally occurring 1:1 aluminosilicate mineral $[\text{Al}_2\text{Si}_2\text{O}_5(\text{OH})_4]$ or $[\text{Al}_2\text{O}_3 \cdot 2\text{SiO}_2 \cdot 2\text{H}_2\text{O}]$ with an anorthic (triclinic) lattice structure composed of one sheet of corner-sharing tetrahedrons and one of Al octahedra. The potential adsorption sites on kaolin include the silanol $\equiv \text{SiOH}$ and aluminol $\equiv \text{AlOH}$ (either at the surface or inside), hydroxyl groups on the mineral edges and the permanently charged sites $\equiv \text{X}^-$ on the basal surface, although such negative charges due to isomorphous substitution are usually very small.

The CEC value of the KT3B sample is 2.7 $\text{cmol}(+)/\text{kg}$, lower than that reported by Miranda-Trevino and Coles (Miranda-Trevino and Coles, 2003); this finding is mainly due to the high amount of illite (27.02%), which is capable of increasing the PZC, CEC and SSA of the kaolin (Tschapek et al., 1974). The grain-size distribution of KT3B was characterized by values typically $< 2 \mu\text{m}$ (Fig. S1 - see the Supplementary Information file); a distribution maximum is observed in the

Table 2
Surface properties of the raw kaolin sample KT3B.

Parameter	Value
Average particle size (μm)	<15
BET specific surface area (m^2/g)	21.27
Total pore volume (mL/g)	0.056
Average pore diameter (μm)	212.38
Density (g/cm^3)	0.6
PZC	6.7
CEC ($\text{cmol}(+)/\text{kg}$)	2.7

2–0.5 μm fraction with about half the total mass.

The BET/ N_2 specific surface area of flakes equaled $21.27 \text{ m}^2/\text{g}$ while their average pore diameter was $212.38 \mu\text{m}$ (Table 2); such values are similar to those given by Zhang et al. (2015). Hence, the MB species can easily enter into the kaolin pores; such a finding can be confirmed by both the polarizing microscope and SEM images (Fig. S2 in the Supplementary information file). As regards the surface morphology of KT3B, SEM data indicate that this kaolin sample presents flaky-shaped particles. The FTIR spectrum revealed (Fig. 2) bands between 3697 cm^{-1} and 3622 cm^{-1} , corresponding respectively to the OH stretching vibrations of the surface and inner Al–OH groups of kaolinite. The bands at 992 cm^{-1} to 1112 cm^{-1} can be ascribed to the stretching vibrations of the Si–O–Si of kaolinite or quartz; the band at 696 cm^{-1} is commonly attributed to out-of-plane Si–O stretching, and that at 798 cm^{-1} to OH deformation linked to Al. The band at 3598 cm^{-1} was attributed to the stretching of the OH bonded to Fe^{3+} , with a slight shoulder at 875 cm^{-1} (strain OH) corresponding to the presence of iron in the kaolinite structure, with Fe^{3+} ions occupying octahedral sites by means of substitution for Al^{3+} cations (Zhang et al., 2015).

3.2. Effect of contact time on MB removal

The adsorption dynamics of the MB solution/KT3B system strongly depend on the contact time. A contact time optimization for the above system was therefore carried out in batch mode. The extent of MB removal by KT3B at different shaking times up to 180 min, while imposing a constant settling time, is shown in Fig. 3. MB adsorption reached a maximum after a very short time of equilibrium, thus suggesting an almost instantaneous MB removal from water. From these data, we selected a contact time of 120 min for all adsorption experiments.

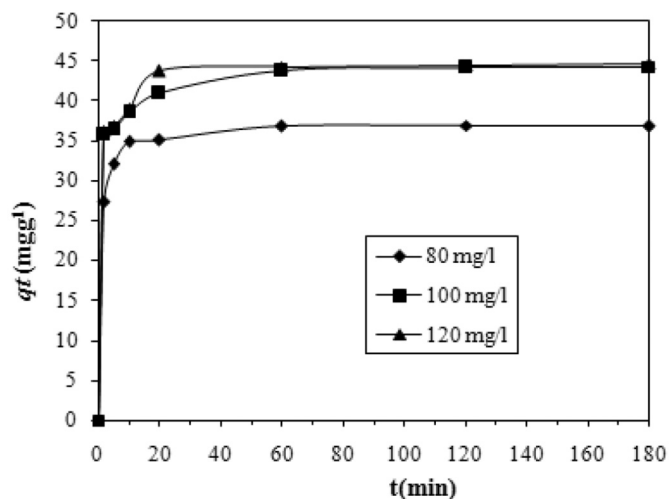


Fig. 3. Effect of initial MB concentration and contact time with regard to MB adsorption onto kaolin at $\text{pH} = 6.0$, $\text{S}/\text{L} = 0.5 \text{ g}/\text{L}$.

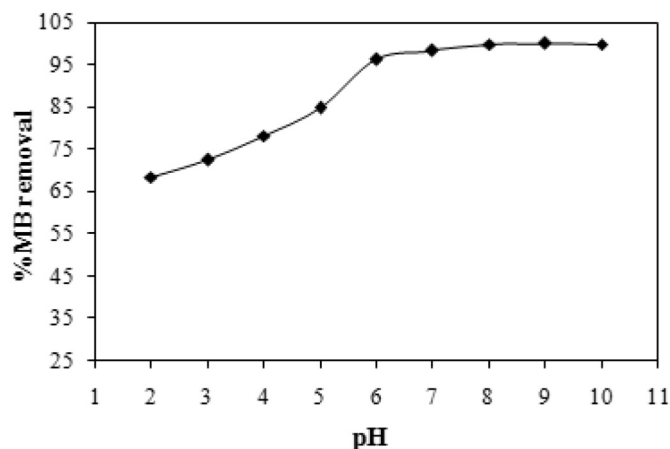


Fig. 4. Effect of pH on MB adsorption on the KT3B kaolin sample at $25 \text{ }^\circ\text{C}$ ($C_0 = 100 \text{ mg}/\text{L}$, $\text{S}/\text{L} = 0.5 \text{ g}/\text{L}$, contact time = 120 min).

3.3. Effect of pH on MB adsorption

The adsorption process is greatly affected by the change in pH of the solution. The effect of solution pH generally depends on the ions present in the reaction mixture as well as on electrostatic interactions with the adsorption surface. Solution pH would influence both aqueous chemistry and surface binding sites of the adsorbents.

The highest adsorption capacity was obtained at $\text{pH} = 9$, while the maximum adsorption efficiency amounted to $99.9 \text{ mg}/\text{g}$ (Fig. 4).

The variation in MB uptake with respect to the initial solution pH can be explained with respect to the point of zero charge (PZC) of KT3B. For the raw kaolin sample, the point of zero charge was measured at 6.7 ± 0.1 . Above this pH value, the kaolin particles acquired negative surface charges, leading to a stronger electrostatic attraction relative to the MB cationic dye. At a pH below PZC, the kaolin surface acquired positive charges and given that the dye molecules also carried a positive charge, an electrostatic repulsion caused a decrease in dye uptake.

3.4. Effect of ionic strength

The effect of ionic strength on dye uptake was studied by adding an NaCl concentration ranging from 0.01 to 0.50 mol/L. An increase in ionic strength resulted in the decrease in MB removal capacity of KT3B (Fig. 5), as had previously been observed by others (Rida et al., 2013). The presence of salt (NaCl) in the solution may have shielded the electrostatic interaction between opposing charges at the solid sorbent surface and on dye molecules, which resulted in the adsorbed amount decreasing with the increase in NaCl concentration (i.e. *salting out*

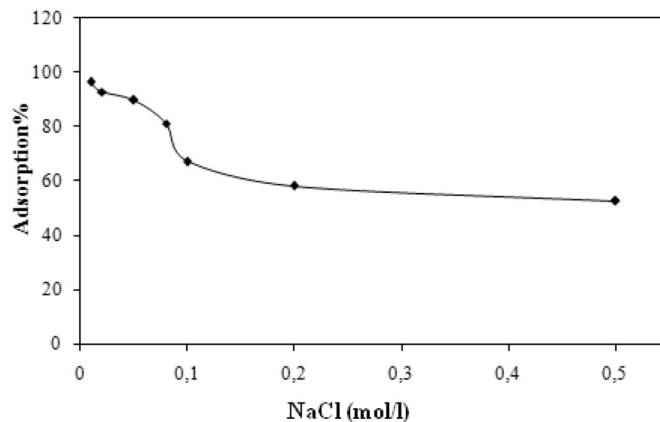


Fig. 5. The effect of ionic strength (NaCl) on dye removal efficiency at $\text{pH} = 6$ ($C_0 = 100 \text{ mg}/\text{L}$, $\text{S}/\text{L} = 0.5 \text{ g}/\text{L}$).

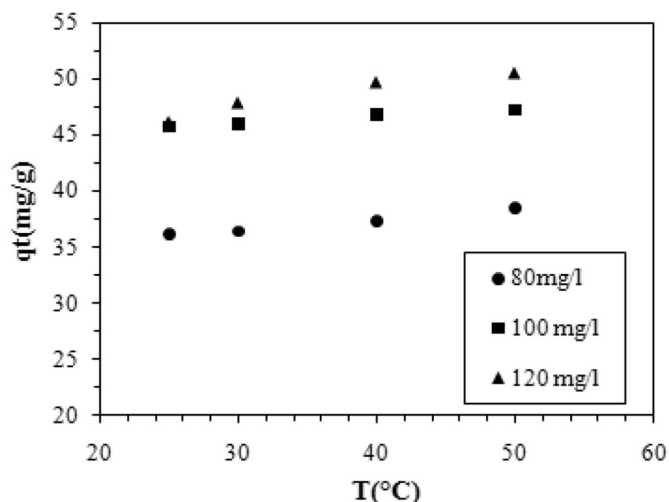


Fig. 6. Influence of temperature on MB dye removal efficiency for KT3B kaolin (adsorbent dosage S/L = 0.5 g/L, pH = 6.0, contact time = 120 min).

effect).

3.5. Effect of temperature

To evaluate the effect of temperature on the adsorption capacities of the kaolin for MB, batch adsorption studies were carried out in the 25–50 °C temperature range. The adsorption capacities of the kaolin for MB increased slightly with an increase in temperature (Fig. 6). This behavior was obvious because as temperature rises, solution viscosity drops, which is favorable to the subsequent adsorption stages: external transfer, and diffusion of adsorbate within the adsorbent solid. This increase may be due to: i) the increase in dye mobility, allowing it to penetrate the sample pores; ii) the increase in chemical interactions between the adsorbate and surface functionalities of the adsorbent; and iii) the change in chemical potentials, correlated with adsorbate species solubility.

3.6. Effect of adsorbent dosage

Several steps were observed (Fig. 7) from the results of experiments with varying adsorbent concentrations (from 0.1 to 1 g/L). Initially, a rapid increase in adsorption with an increase in adsorbent quantity can be attributed to a greater surface area and the availability of more adsorption sites. Beginning with an adsorbent concentration equal to

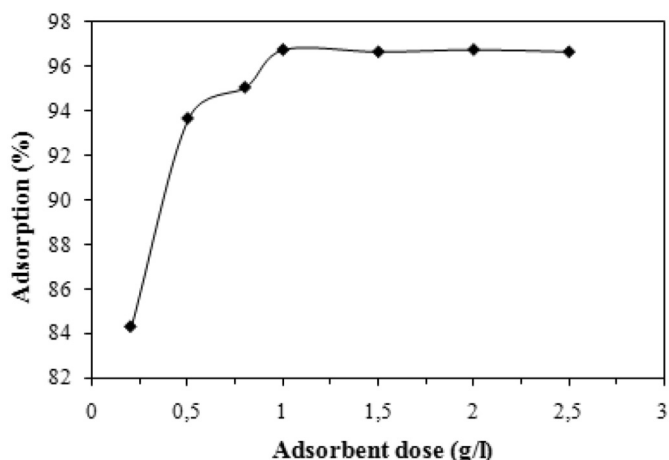


Fig. 7. Effect of adsorbent concentration on the MB adsorption percentage, C₀ = 100 mg/L.

0.5 g/L, at which point approx. 97.5% of the dye becomes adsorbed, the adsorption rate was gradually lowered until reaching a maximum value of around 97% adsorption. Thus, an optimal KT3B dosage for MB adsorption was found to be 1.0 g/L. All active sites on the adsorbent surface were then occupied, and any increase in adsorbent dosage did not yield a higher MB uptake.

3.7. Kinetic studies

We first of all investigated the kinetics of adsorption, which is critical to process efficiency. Two well-known adsorption kinetic models were used in this work: the pseudo-first order Lagergren equation and the pseudo-second order rate equation were both fitted with the experimental data (Limousin et al., 2007).

The pseudo-first order equation is based on the assumption that the rate of change in solute adsorption over time is directly proportional to the difference in saturation concentration and the amount of adsorptive solid uptake over time (Ho, 2004). The corresponding differential equation is written as:

$$dq_t/dt = k_1 (q_e - q_t) \tag{5}$$

Integrating Eq. (5) for the boundary conditions $t = 0$ to $t = t$ and $q_t = 0$ to $q_t = q_t$ yields:

$$\ln(q_e - q_t) = \ln q_e - k_1 t \tag{6}$$

Let's note that k_1 and q_e can be determined from the slope and intercept of the plots of $\ln(q_e - q_t)$ vs. t for various experimental conditions.

The removal data were also analyzed by the pseudo-second order kinetic model, expressed as follows (Ho, 2006):

$$dq_t/dt = k_2 (q_e - q_t)^2 \tag{7}$$

Integrating Eq. (7), using the boundary conditions at $t = 0$, $q_t = 0$ and for any time t , with the amount of dye adsorbed being q_t and in rearranging the corresponding rate law, generates:

$$q_t = k_2 q_e^2 t / (1 + k_2 q_e t) \tag{8}$$

In Eq. (8), k_2 (g/(mg.min)) is the pseudo-second order rate constant, and q_e and q_t (mg/g) are the values of the amount adsorbed per unit mass at equilibrium and at any time t , respectively.

The first-order kinetic curves from this study did not fit well with the experimental data (not shown). The pseudo-second order equation however did provide an excellent fit (Fig. 8), with a regression coefficient $R^2 \geq 0.99$ for all systems and a favorable value of RMSE (Table 3). The calculated q_e values from the model were also in good agreement with experimental values (Table 3). The kinetics of MB sorption on the KT3B sorbent thus follow the pseudo-second order rate expression.

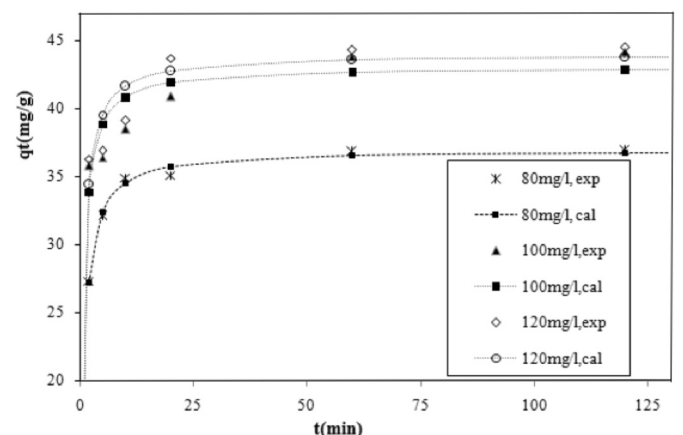


Fig. 8. Pseudo-second order plots for the adsorption of MB onto KT3B at various initial concentrations, pH = 6.0, S/L = 0.5 g/L, T = 25 °C.

Table 3
Kinetic parameters involved in MB removal by KT3B (pH = 6.0, T = 25 °C).

C ₀ (mg/L)	k ₂ (g/mgmin)	Pseudo 2nd order model			
		q _{e, (exp)} (mg/g)	q _{e, (cal)} (mg/g)	R ²	RMSE
80	0.037	36.80	36.98	0.997	0.333
100	0.042	42.90	43.03	0.991	1.727
120	0.040	44.7	43.96	0.986	1.686

3.8. Isotherm experiments

An adsorption isotherm describes the equilibrium between adsorbent and adsorbate, i.e. in this case the relationship between the quantity of dye adsorbed and that remaining in aqueous solution at a fixed temperature at equilibrium. The isotherm thus yields a number of parameters whose values express the surface properties and affinity of the adsorbent. In order to optimize the design of an adsorption system to remove dyes from effluents, it is important to establish the most appropriate correlation for the equilibrium data.

The Langmuir isotherm equation (Limousin et al., 2007), which assumes a monolayer sorption of dye molecules on the sorbent surface, is expressed as follows:

$$q_e = q_{max} K_L C_e / (1 + K_L C_e) \tag{9}$$

where q_e is the adsorbed amount of dye at equilibrium (mg/g), C_e the equilibrium concentration of the dye in solution (mg/L), q_{max} the maximum adsorption capacity (mg/g), and K_L the constant related to the free energy of adsorption (L/mg). According to the plot of experimental data at different pH values (Fig. 9), the Langmuir isotherm model was found to fit closely with these experimental data, as witnessed by the coefficient of determination R² in Table 4. The other two statistical parameters (χ² and RMSE) also confirmed the quality of this fit.

One essential characteristic of the Langmuir equation can be expressed in terms of the dimensionless factor R_L (Hall separation factor), which is calculated (Weber and Chakravorti, 1974) as follows:

$$R_L = 1 / (1 + K_L C_e) \tag{10}$$

where K_L is the Langmuir constant (L/mg) and C₀ the initial MB concentration (mg/L); R_L is indicative of the isotherm shape and predicts whether a sorption system is favorable (0 < R_L < 1) or unfavorable (R_L > 1).

In the present study, the calculated R_L values for the adsorption of

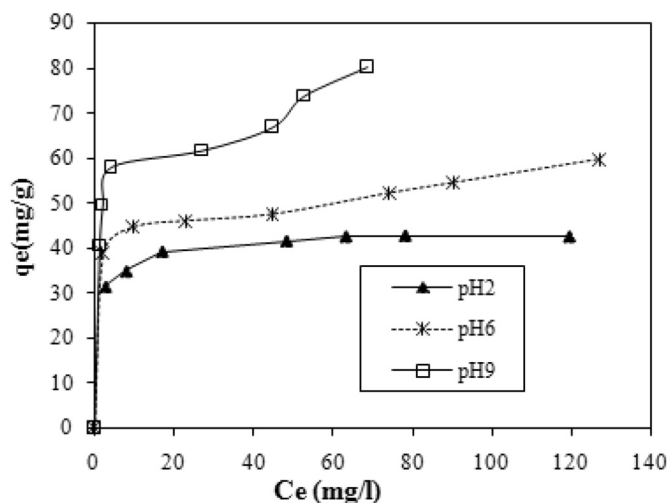


Fig. 9. The Langmuir adsorption isotherm for MB adsorption on KT3B (adsorbent dosage: 0.5 g/L, T = 25 °C), as a nonlinear expression.

Table 4
Parameters of Langmuir isotherm for MB adsorption onto KT3B kaolin (T = 25 °C).

pH	q _{max} (mg/g)	K _L (L/g)	R ²	χ ²	RMSE
2	42.60	0.84	0.997	0.218	1.028
6	52.76	1.04	0.975	0.407	3.47
9	72.57	0.96	0.980	0.361	2.67

MB on the KT3B kaolin sample were found to equal 0.0118, 0.0094, 0.0079 and 0.0063 at initial concentrations of 80, 100, 120 and 150 mg/L, respectively. These R_L values confirmed that KT3B is favorable for adsorbing MB from water under the conditions applied in this study.

3.9. Thermodynamic analyses

Thermodynamic parameters, including Gibbs free energy change (ΔG°), enthalpy change (ΔH°) and entropy change (ΔS°), serve to evaluate the effect of temperature on the adsorption of MB onto kaolin and provide in-depth information regarding the inherent energy changes associated with the adsorption process (Salvestrini et al., 2014). These parameters are calculated from the following equation:

$$\Delta G^\circ = -RT \text{Ln } K_L^\circ \tag{11}$$

where R is the universal gas constant (8.314 J/mol K), T the temperature (K), and K_L[°] the (dimensionless) ‘thermodynamic’ Langmuir constant for the adsorption process. To obtain this value from the value K_L (in L/mg) calculated from isotherm data (see Section 3.8), we had to change all concentrations to molar form and take into account the standard state C° = 1 mol/L (Salvestrini et al., 2014; Zhou and Zhou, 2014):

$$K_L^\circ = K_L \text{ (L/mg)} \times 1000 \text{ (mg/g)} \times M_{MB} \text{ (g/mol)} \times C^\circ \text{ (mol/L)} \tag{12}$$

where M_{MB} = 319.85 g/mol is the MB molar mass, and the factor 1000 allows converting g to mg.

The enthalpy (ΔH°) and entropy (ΔS°) parameters were estimated from the classical relationships:

$$\text{Ln } K_L^\circ = (\Delta S^\circ / R) - (\Delta H^\circ / RT) \tag{13}$$

$$\Delta G^\circ = \Delta H^\circ - T \Delta S^\circ \tag{14}$$

The plot of LnK_L[°] versus 1/T yielded a straight line (Fig. S3 in the Supplementary Information file), and the values of ΔH° (kJ/mol) and ΔS° (J/mol K) can be calculated from the intercept and slope of these Van 't Hoff plots, respectively. The values of ΔG° (kJ/mol) were recalculated from ΔH° and ΔS° (see Table 5). The positive values of ΔH° are indicative of an endothermic adsorption process; both ΔH° and ΔS° decreased with an increase in pH. The negative values of ΔG° were

Table 5
Thermodynamic parameters for MB adsorption on KT3B.

pH	T (K)	K _L (L/mg)	K _L [°] (dimensionless)	LnK _L [°]	ΔG° (kJ/mol)	ΔH° (kJ/mol)	ΔS° (J/mol K)
2	298	0.84	268674	12.50	-31.90	25.08	191.22
	303	1.03	329445.5	12.70	-32.85		
	313	1.18	377423	12.84	-34.76		
6	323	1.47	470179.5	13.06	-36.68	17.11	163.28
	298	1.04	332644	12.71	-31.54		
	303	1.27	406209.5	12.91	-32.36		
9	313	1.47	470179.5	13.06	-33.99	16.51	159.62
	323	1.85	591722.5	13.29	-35.62		
	298	1.17	376143.6	12.83	-31.05		
	303	1.57	502164.5	13.12	-31.85		
13	313	2.00	641299.25	13.37	-33.45		
	323	2.71	866793.5	13.67	-35.04		

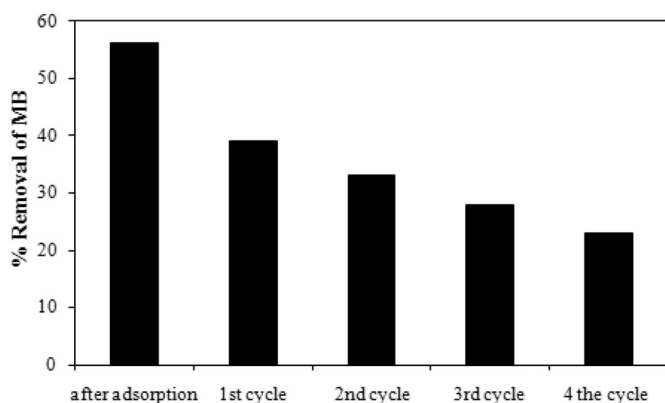


Fig. 10. Effect of desorption cycles on MB removal (adsorbent dosage = 0.5 g/L, dye solution pH = 6.0).

Table 6
Maximum loading capacity (Langmuir model) for MB on selected clayey materials.

Adsorbent	Capacity (mg/g) at given T (°C)	Reference
Montmorillonite	289.12 (35 °C)	Almeida et al. (2009)
Natural clay (Turkey)	58.2 (20 °C)	Gürses et al. (2006)
Ball clay (Malaysia)	Raw 25.01 Modified 62.50 (30 °C)	Auta and Hameed (2012)
Kaolinite	45.45	Sarma et al. (2011)
Montmorillonite	163.93 (30 °C)	
Kaolin (Persia)	28.95 (25 °C)	Tehrani-Bagha et al. (2011)
Natural zeolite	21.78 (30 °C)	Wang and Zhu (2006)
Natural clay (Portugal)	22.2	Hajjaji et al. (2016)
Commercial kaolin	23.1 (20 °C)	
Raw coal-bearing kaolin	78.1	Gao et al. (2016)
Acid-activated kaolin	101.5 (22 °C)	
Zeolites from kaolin (Egypt)	11.13 to 21.41 (25 °C) ^a	El-Mekkawi et al. (2016)
Kaolin	Raw 13.99 Pure 15.55 (RT) ^b	Ghosh and Bhattacharyya (2002)
Kaolinite	102.04 (25 °C)	Krishnan et al. (2015)
Raw KT3B kaolin (Algeria)	52.76 (25 °C)	Present study

^a According to sample.

^b RT = at room temperature.

found to slightly increase as temperature increases from 298° to 323 K. Negative ΔG° values confirmed the feasibility and spontaneity of the adsorption process.

3.10. Desorption studies

Recycling the adsorbent is considered to be an important economic aspect in minimizing material costs. Since the present study was undertaken within the framework of a sustainable development approach, we decided to limit our desorption tests to water rinses only. The use of chemical reagents would indeed be more efficient, but such an approach would simultaneously produce potentially hazardous leachates, which would need to be disposed of properly and, hence, outside the scope of our project.

The adsorption/desorption experimental cycles were carried out up to three times. After four cycles, the adsorption capacity of MB on adsorbent decreased from 56% to 23% (Fig. 10). This behavior indicates that the adsorbent can successfully hold MB after its adsorption from aqueous solution.

3.11. Comparison of adsorption capacity with other available adsorbents

The adsorption capacity of KT3B kaolin was compared with a selection of other clayey adsorbents (Table 6). These data clearly

demonstrated that the present raw kaolin KT3B sample adsorbent was effective in the removal of MB dye from the aqueous phase and, as expected, compared well with other clay materials.

4. Conclusion

The selected raw kaolin KT3B sample proved to be an effective adsorbent for the removal of MB from aqueous solution. The percentage of adsorption was maximal at a pH value of 9.0 and decreased in more acidic MB solutions. At an initial dye concentration of 100 mg/L, the percentage of adsorption decreased from about 98% to 68% as pH dropped from 10 to 2. The adsorption equilibrium was attained within times of < 30 min. The adsorption kinetics was well described by the pseudo-second order model equation. An adsorption isotherm was fitted by the Langmuir model, with the maximum adsorption capacity of MB on KT3B was calculated at 52.76 mg/g at 25 °C and pH = 6. These results also revealed that the process was more efficient at higher temperatures. The thermodynamic activation parameters showed that the process was endothermic.

Our results therefore indicate that a raw kaolin sample, like the KT3B used in this work, can be successfully utilized for the adsorption of Methylene Blue dye from aqueous solutions.

Disclosure statement

No potential conflict of interest was reported by the authors.

Funding

This research did not receive any specific grant from funding agencies in the public, commercial, or not-for-profit sectors.

Appendix A. Supplementary data

Supplementary data to this article can be found online at <https://doi.org/10.1016/j.clay.2017.11.034>.

References

- Allègre, C., Moulin, P., Maisseu, M., Charbit, F., 2006. Treatment and reuse of reactive dyeing effluents. *J. Membr. Sci.* 269, 15–34.
- Almeida, C.A.P., Debacher, N.A., Downs, A.J., Cottet, L., Mello, C.A.D., 2009. Removal of methylene blue from colored effluents by adsorption on montmorillonite clay. *J. Colloid Interface Sci.* 332, 46–53.
- Au, P.I., Leong, Y.K., 2013. Rheological and zeta potential behaviour of kaolin and bentonite composite slurries. *Colloids Surf. A* 436, 530–541.
- Auta, M., Hameed, B.H., 2012. Modified mesoporous clay adsorbent for adsorption isotherm and kinetics of methylene blue. *Chem. Eng. J.* 198–199, 219–227.
- Bouzerara, F., Boulanacer, S., Harabi, A., Boudaira, B., Achour, S., 2009. Preparation and characterization of macroporous ceramic supports for membranes. *Phys. Procedia* 2, 1449–1453.
- Chen, J., Anandarajah, A., Inyang, H., 2000. Pore fluid properties and compressibility of kaolinite. *J. Geotech. Geoenviron. Eng.* 126, 798–807.
- Crini, G., 2006. Non-conventional low-cost adsorbents for dye removal: a review. *Bioresour. Technol.* 97, 1061–1085.
- DiSanto, A.R., Wagner, J.G., 1972. Pharmacokinetics of highly ionized drugs I: methylene blue – whole blood, urine and tissue assays. *J. Pharm. Sci.* 61, 598–602.
- El-Mekkawi, D.M., Ibrahim, F.A., Selim, M.M., 2016. Removal of methylene blue from water using zeolites prepared from Egyptian kaolins collected from different sources. *J. Environ. Chem. Eng.* 4, 1417–1422.
- Gadd, G.M., 2009. Biosorption: critical review of scientific rationale, environmental importance and significance for pollution treatment. *J. Chem. Technol. Biotechnol.* 84, 13–28.
- Gao, W., Zhao, S., Wu, H., Deligeer, W., Asuha, S., 2016. Direct acid activation of kaolinite and its effects on the adsorption of methylene blue. *Appl. Clay Sci.* 126, 98–106.
- Ghosh, D., Bhattacharyya, K.G., 2002. Adsorption of methylene blue on kaolinite. *Appl. Clay Sci.* 20, 295–300.
- Gupta, S.S., Bhattacharyya, K.G., 2012. Adsorption of heavy metals on kaolinite and montmorillonite: a review. *Phys. Chem. Chem. Phys.* 14, 6698–6723.
- Gupta, V.K., Suhas, 2009. Application of low-cost adsorbents for dye removal – a review. *J. Environ. Manag.* 90, 2313–2342.
- Gürses, A., Dogar, C., Yalçın, M., Açıkıldız, M., Bayrak, R., Karaca, S., 2006. The adsorption kinetics of the cationic dye methylene blue onto clay. *J. Hazard. Mater.* B131, 217–228.

- Hajjaji, W., Andrejkovičová, S., Pullar, R.C., Tobaldi, D.M., Lopez-Galindo, A., Jammoussi, F., Rocha, F., Labrincha, J.A., 2016. Effective removal of anionic and cationic dyes by kaolinite and TiO₂/kaolinite composites. *Clay Miner.* 51, 19–27.
- Hang, P.T., Brindley, G.W., 1970. Methylene blue absorption by clay minerals. Determination of surface areas and cation exchange capacities [clay-organic studies XVIII]. *Clays Clay Miner.* 18, 203–212.
- Hao, O.J., Kim, H., Chiang, P.C., 2000. Decolorization of wastewater. *Crit. Rev. Environ. Sci. Technol.* 30, 449–505.
- Harris, R.G., Wells, J.D., Johnson, B.B., 2001. Selective adsorption of dyes and other organic molecules to kaolinite and oxide surfaces. *Colloids Surf. A Physicochem. Eng. Asp.* 180, 131–140.
- Ho, Y.S., 2004. Citation review of Lagergren kinetic rate equation on adsorption reactions. *Scientometrics* 59, 171–177.
- Ho, Y.S., 2006. Review of second-order models for adsorption systems. *J. Hazard. Mater.* B136, 681–689.
- Holkar, C.R., Jadhav, A.J., Pinjari, D.V., Mahamuni, N.M., Pandit, A.B., 2016. A critical review on textile wastewater treatments: possible approaches. *J. Environ. Manag.* 182, 351–366.
- Kannan, N., Sundaram, M.M., 2001. Kinetics and mechanism of removal of methylene blue by adsorption on various carbons – a comparative study. *Dyes Pigments* 51, 25–40.
- Krishnan, K.A., Ajmal, K., Faisal, A.K., Liji, T.M., 2015. Kinetic and isotherm modeling of methylene blue adsorption onto kaolinite clay at the solid-liquid interface. *Sep. Sci. Technol.* 50, 1147–1157.
- Limousin, G., Gaudet, J.P., Charlet, L., Szenknect, S., Barthès, V., Krimissa, M., 2007. Sorption isotherms: a review on physical bases, modelling and measurement. *Appl. Geochem.* 22, 249–275.
- Marrot, B., Roche, N., 2002. Wastewater treatment and reuse in textile industries, a review. *Res. Adv. Water Res.* 3, 41–53.
- Miranda-Trevino, C., Coles, C.A., 2003. Kaolinite properties, structure and influence of metal retention on pH. *Appl. Clay Sci.* 23, 133–139.
- Mondal, S., 2008. Methods of dye removal from dye house effluent: an overview. *Environ. Eng. Sci.* 25, 383–396.
- Ngulube, T., Ray Gumbo, J., Masindi, V., Maity, A., 2017. An update on synthetic dyes adsorption onto clay based minerals: a state-of-art review. *J. Environ. Manag.* 191, 35–57.
- Noh, J.S., Schwarz, J.A., 1989. Estimation of the point of zero charge of simple oxides by mass titration. *J. Colloid Interface Sci.* 130, 157–164.
- Oz, M., Lorke, D.E., Hasan, M., Petronaiou, G.A., 2010. Cellular and molecular actions of methylene blue in the nervous system. *Med. Res. Rev.* 31, 93–117.
- Pansu, M., Gautheyrou, J., 2003. *L'analyse du sol: minéralogique, organique et minérale*. Springer, Paris.
- Pelekani, C., Snoeyink, V.L., 2000. Competitive adsorption between atrazine and methylene blue on activated carbon: the importance of pore size distribution. *Carbon* 38, 1423–1436.
- Primo-Yúfera, E., Carrasco Dorrién, J.M., 1981. *Química Agrícola*. vol. 1 Alhambra, Barcelona.
- Quintelas, C., Figueiredo, H., Tavares, T., 2011. The effect of clay treatment on remediation of diethylketone contaminated wastewater: uptake, equilibrium and kinetic studies. *J. Hazard. Mater.* 186, 1241–1248.
- Rafatullah, M., Sulaiman, O., Hashim, R., Ahmad, A., 2010. Adsorption of methylene blue on low-cost adsorbents: a review. *J. Hazard. Mater.* 177, 70–80.
- Raposo, F., De La Rubia, M.A., Borja, R., 2009. Methylene blue number as useful indicator to evaluate the adsorptive capacity of granular activated carbon in batch mode: influence of adsorbate/adsorbent mass ratio and particle size. *J. Hazard. Mater.* 165, 291–299.
- Rida, K., Bouraoui, S., Hadnine, S., 2013. Adsorption of methylene blue from aqueous solution by kaolin and zeolite. *Appl. Clay Sci.* 83–84, 99–105.
- Rodríguez, A., Ovejero, G., Mestanza, M., García, J., 2012. Dyes adsorption on low cost adsorbents: inorganic materials. *Desal. Water Treat.* 45, 191–205.
- Salvestrini, S., Leone, V., Iovino, P., Canzano, S., Capasso, S., 2014. Considerations about the correct evaluation of sorption thermodynamic parameters from equilibrium isotherms. *J. Chem. Thermodyn.* 68, 310–316.
- Sánchez-Jiménez, N., Sevilla, M.T., Cuevas, J., Rodríguez, M., Procopio, J.R., 2012. Interaction of organic contaminants with natural clay type geosorbents: potential use as geologic barrier in urban landfill. *J. Environ. Manag.* 95, S182–S187.
- Sanchez-Martin, M.J., Rodriguez-Cruz, M.S., Andrades, M.S., Sanchez-Camazano, M., 2006. Efficiency of different clay minerals modified with a cationic surfactant in the adsorption of pesticides: influence of clay type and pesticide hydrophobicity. *Appl. Clay Sci.* 31, 216–228.
- Sarma, G.K., SenGupta, S., Bhattacharyya, K.G., 2011. Methylene blue adsorption on natural and modified clays. *Sep. Sci. Technol.* 46, 1602–1614.
- Schroeder, P.A., Erickson, G., 2014. Kaolin: from ancient porcelains to nanocomposites. *Elements* 10, 177–182.
- Tehrani-Bagha, A.R., Nikkar, H., Mahmoodi, N.M., Markazi, M., Menger, F.M., 2011. The sorption of cationic dyes onto kaolin: kinetic, isotherm and thermodynamic studies. *Desalination* 266, 274–280.
- Tschapek, M., Tcheichvili, L., Wasowski, C., 1974. The point of zero charge (pzc) of kaolinite and SiO₂ + Al₂O₃ mixtures. *Clay Miner.* 10, 219–229.
- Vimonses, V., Lei, S., Jin, B., Chow, C.W.K., Saint, C., 2009. Adsorption of congo red by three Australian kaolins. *Appl. Clay Sci.* 43, 465–472.
- Walsh, G.E., Bahner, L.H., Horning, W.B., 1980. Toxicity of textile mill effluents to freshwater and estuarine algae, crustaceans and fishes. *Environ. Pollut. Ser. A. Ecol. Biol.* 21, 169–179.
- Wang, S., Zhu, Z.H., 2006. Characterisation and environmental application of an Australian natural zeolite for basic dye removal from aqueous solution. *J. Hazard. Mater.* B136, 946–952.
- Weber, T.W., Chakravorti, R.K., 1974. Pore and solid diffusion models for fixed-bed adsorbents. *AICHE J.* 20, 228–238.
- Yagub, M.T., Sen, T.K., Afroze, S., Ang, H.M., 2014. Dye and its removal from aqueous solution by adsorption: a review. *Adv. Colloid Interf. Sci.* 209, 172–184.
- Zhang, H., Niu, Z., Liu, Z., Wen, Z., Li, W., Wang, X., Wu, W., 2015. Equilibrium, kinetic and thermodynamic studies of adsorption of Th(IV) from aqueous solution onto kaolin. *J. Radioanal. Nucl. Chem.* 303, 87–97.
- Zhou, X., Zhou, X., 2014. The unit problem in the thermodynamic calculation of adsorption using the Langmuir equation. *Chem. Eng. Comm.* 201, 1459–1467.